

Automatic Detection of Cerebral Microbleed in SWI using Radon Transform

Amir Fazlollahi^{1,2}, Fabrice Meriaudeau², Luca Giancardo^{2,3}, Patricia M Desmond⁴, Victor L Villemagne⁵, Christopher C Rowe⁵, Paul Yates⁵, Olivier Salvado¹, Bourgeat Pierrick¹, and the AIBL Research Group⁶

¹The Australian E-Health Research Centre-BioMedIA, Brisbane, QLD, Australia, ²Laboratoire Le2I, Université de Bourgogne, Le Creusot, France, ³Istituto Italiano di Tecnologia, Genoa, Italy, ⁴Department of Radiology, The Melbourne Brain Centre at Royal Melbourne Hospital, University of Melbourne, Melbourne, VIC, Australia, ⁵Department of Nuclear Medicine and Centre for PET, Austin Hospital, Melbourne, VIC, Australia, ⁶<http://www.aibl.csiro.au/>, Australia, Australia

Introduction: Susceptibility-weighted imaging (SWI) has improved the sensitivity in the identification of small Cerebral Microbleed (CMB) which is linked with normal aging, manifestation/progression of cerebrovascular disease and dementia^{1,2}. Since presence and number of CMBs have come to attention as a potential diagnostic and prognostic biomarker, an automated scheme to improve visualization is required. This would augment visual rating by human expert which is time consuming, non-reproducible and prone to inter-reader variability as CMBs may vary in size (2-10mm) and contrast. Furthermore, using T2* contrast, CMBs can easily be mistaken by vessel's cross-sections in SWIs. CMB read depends on the pulse sequence, its parameters, resolution and magnetic field strength but generally appear as hypo-intense, nearly spherical structure on MRI due to local susceptibility effect when exposed to MR magnetic field.

So far, few methods have been proposed for CMB identification using Radial Symmetry Transform³, shape features along with classifier⁴ or unified segmentation-normalization model⁵. All of the current methods suffer from low sensitivity and specificity and perform poorly on small, low contrast CMBs. The best achieved result had maximum sensitivity of 81.7%, specificity of 95% and very high false-positive rate⁴.

In this study, a new approach of microbleed identification in SWIs is presented and compared to visual rating. The method relies on two main steps: (1) a 3D anisotropic multi-scale approach extracts size and centre of all potential CMBs within the image, and (2) feature extraction using the Radon transform for final classification using a random forest (RF) classifier. The novelty of the technique consists in combining Radon transform and multi-scale analysis to obtain robust feature descriptors.

Method: For this study, a subset of 30 AD/MCI subjects with CMBs from the Australian Imaging Biomarkers and Lifestyle (AIBL) study were included. For each subject, anatomical T1-weighted MPRage and SWI images are available. 3D SWI was acquired on a 3-T Siemens TRIO scanner with 0.9x0.9 mm in-plane resolution and 1.75 mm slice thickness, repetition time/echo time of 27/20 msec, and flip angle 20°. One expert had reviewed SWI images and in total 64 CMBs with prevalence of 2.1±2.2 per subject were found. For each subject, the T1W MPRage was segmented using an expectation maximization algorithm to generate a brain mask. The dynamic intensity range of SWI was normalized to [0,1] after trimming the top 1% of intensity values within the brain mask. The image was then inverted so that CMBs and vessels appear hyperintense. For pre-screening phase, a 3D multi-scale Laplacian of Gaussian (trace of Hessian matrix) filter is performed to identify potential CMBs of varying size (2-10mm). This filter, which uses a range of σ (standard deviation), extracts local minimas as points of interest and sphericity was then assessed via eigenvalue analysis of the obtained Hessian matrix where three large negative values are expected. Small CMBs do not necessarily appear spherical due to partial volume effect and voxel anisotropy, and therefore the ratio of two highest eigenvalues is considered as decision threshold. This approach also allows defining a 3D patch around each candidate CMB since both size (relative to σ) and center are estimated.

Radon transform in which shape, size and intensity are combined is used as the preferred domain for feature extraction. Radon can effectively transform 3D dimensional image by accumulating the intensity along a plane oriented for a given set of angles. The resulting projection is the sum of the intensities in each direction, highlighting spherical structures even when noise and vessels are present. Spherical objects appear as a continuous chain of cliffs in Radon space⁶ (Figure 1). The selected features are the first derivative of the mean, and the standard deviations computed across each Radon angle-dimension (Figure 2). The proposed descriptor is invariant to rotation by nature as the Radon is computed on different orientations: $(\theta, \phi) \in [0:5:175]$. Intensity shift invariance is achieved by normalizing each 3D patch by its mean and standard deviation. Scale invariance is obtained by up-sampling the descriptors to a fixed length.

A random forest (RF) classifier was then trained and tested on the potential CMB set using leave-one-out validation scheme.

Results: The pre-screening step has a very high sensitivity of 95%, leaving 3 undetected CMBs out of 64. Upon inspection, these 3 CMBs have irregular shapes and are touching vessels or CSF. At this point the specificity is relatively low and the RF model is able to discard most of the false-positives focusing on maximizing both sensitivity and specificity. The full process had an overall sensitivity of 92% and specificity of 91% producing on average 6.2 false-positives per true CMB and 13.3 CMBs per subject. The algorithm is implemented in Matlab and the whole process takes 3 minutes per subject on a single core machine. The results are summarized in Table 1.

Discussion: In this work, CMB detection on SWI scans based on Radon Transform is presented. Radon-based features along with a multi-scale analysis show promising performance improvement in terms of sensitivity and specificity and compare favorably to previously published methods. The method described in⁴ had sensitivity of 81.7%, specificity of 95% and on average identified 107 CMBs per subject, whereas the method presented in³ had sensitivity of 71.2% producing 17.2 CMBs per subject.

The pre-screening step is flexible to identify very small and low contrast CMBs consisting of few voxels but is still problematic if CMB is touching other structures. As a future work, further global preprocessing such as bias field correction and local contrast enhancement are required. The classifier can be further improved by including more CMBs in the training set and combining Radon-based features with other discriminative shape descriptors.

References: 1. P. Yates, R. Sirisriro, VL Villemagne, et al. Cerebral microhemorrhage and brain β -amyloid in aging and alzheimer disease. *Neurology*, 77(1):48-54, 2011. 2. G. Roob, R. Schmidt, P. Kapeller, A. Lechner, et al. MRI evidence of past cerebral microbleeds in a healthy elderly population. *Neurology*, 52(5):991-991, 1999. 3. H.J. Kuijff, J. de Bresser, M.I. Geerlings, et al. Efficient detection of cerebral microbleeds on 7.0 T MR images using the radial symmetry transform. *NeuroImage*, 2011. 4. S.R.S. Barnes, E.M. Haacke, M. Ayaz, et al. Semiautomated detection of cerebral microbleeds in magnetic resonance images. *Magnetic Resonance Imaging*, 2011. 5. M.L. Seghier, M.A. Kolanko, A.P. Leff, H.R. Jäger, et al. Microbleed detection using automated segmentation (midas): a new method applicable to standard clinical MR images. *PLoS one*, 6(3):e17547, 2011. 6. L. Giancardo, F. Meriaudeau, T.P. Karnowski, et al. Microaneurysm Detection with Radon Transform Based Classification on Retina Images. *EMBC IEEE*, 2011

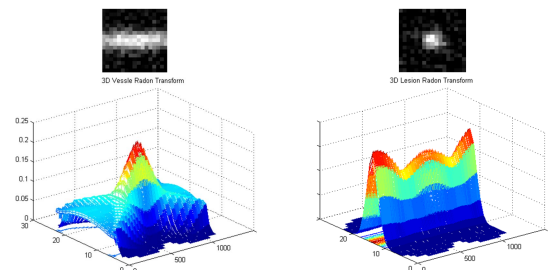


Figure 1. The top row shows a cross-section of synthetic vessel (left) and CMB (right) and the bottom row shows normalized 3D Radon transform of the objects.

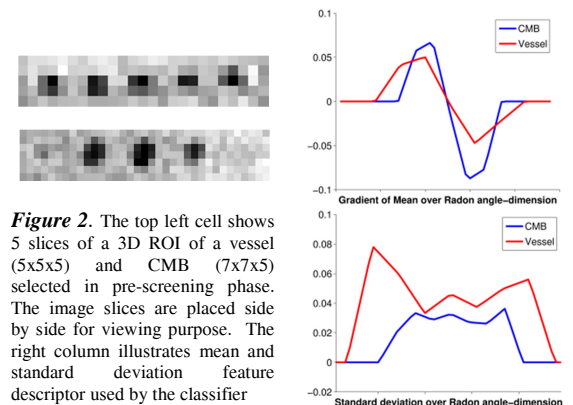


Figure 2. The top left cell shows 5 slices of a 3D ROI of a vessel (5x5x5) and CMB (7x7x5) selected in pre-screening phase. The image slices are placed side by side for viewing purpose. The right column illustrates mean and standard deviation feature descriptor used by the classifier

	Manual identification	Pre-screening	Final result
True-positive	64	61	56
False-positive	-	-	345
False-negative	-	3	5
True-negative	-	4021	3676
Sensitivity	100 %	95 %	92 %
specificity	100 %	-	91 %